THE JOURNAL OF PHYSICAL CHEMISTRY C

Article

pubs.acs.org/JPCC

Physicochemical Properties of Binary Ionic Liquid–Aprotic Solvent Electrolyte Mixtures

Eric T. Fox,[†,§] Elie Paillard,[†,§] Oleg Borodin,[‡] and Wesley A. Henderson*[,†]

[†]Ionic Liquids & Electrolytes for Energy Technologies (ILEET) Laboratory, Department of Chemical & Biomolecular Engineering, North Carolina State University, Raleigh, North Carolina 27695, United States

[‡]Electrochemistry Branch, Sensor & Electron Devices Directorate, U.S. Army Research Laboratory, Adelphi, Maryland 20783, United States

Supporting Information

ABSTRACT: The properties of mixtures of ionic liquids (ILs) with a variety of different aprotic solvents have been examined in detail. The ILs selected—bis(trifluoromethanesulfonyl)imide ($TFSI^-$) salts with *N*-methyl-*N*-pentylpyrrolidinium (PY_{15}^+), -piperidinium (PI_{15}^+), or -morpholinium (MO_{15}^+) cations—enabled the investigation of how cation structure influences the mixture properties. This study includes the characterization of the thermal phase behavior of the mixtures and volatility of the solvents, density and excess molar volume, and transport properties (viscosity and conductivity). The mixtures with ethylene carbonate form a simple eutectic, whereas those with ethyl butyrate appear to form a new IL–solvent crystalline phase. Significant differences in the viscosity of the mixtures are found for different solvents, especially for the IL-rich concentrations. In contrast, only minor differences are noted for the conductivity with different solvents for the IL-rich concentrations. For the solvent-rich concentrations, however, substantial differences are noted in the conductivity, especially for the mixtures with acetonitrile.

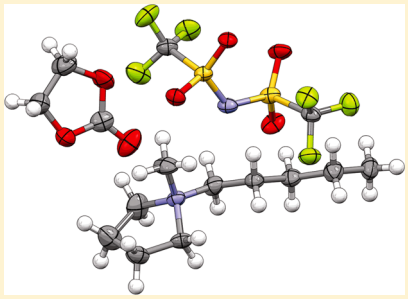

1. INTRODUCTION

Ionic liquids (ILs) have garnered considerable interest as electrolyte materials for a wide range of electrochemical technologies—including batteries, fuel cells, organic dye-sensitized solar cells, actuators, smart windows, and more—due to the combination of favorable properties that many ILs possess such as high electrochemical/thermal stability, wide liquid range, low flammability, and nonvolatility at ambient pressure.[1−6] ILs are salts, or mixtures of salts, which melt at low temperature—often well below ambient temperature. The conductivity of ILs, especially at lower temperatures, is frequently low enough, however, to preclude their use in commercial devices. The introduction of a solvent to the ILs provides a facile means of tuning the properties, including the conductivity, of IL-based electrolytes for specific applications. Notably, IL–solvent mixtures often have much improved properties over similar salt–solvent mixtures. For example, a given IL may be completely miscible in the aprotic solvents typically used for electrolytes (e.g., propylene carbonate), in contrast with high melting tetraalkylammonium salts (e.g., Me_4NBF_4, Et_4NBF_4, etc.) which have limited solubility, permitting the optimized selection of the electrolyte salt concentration.[7] IL–solvent mixtures also often have a higher ionic conductivity and superior device performance at low temperature than comparable mixtures with high melting salts.[7,8]

How the choice of solvent affects the electrolyte properties is not yet well understood, despite many studies devoted to IL–solvent mixtures.[8−25] In addition to solvent (and ion) structure, compositional variations also significantly impact properties. Thus, the physicochemical properties of mixtures composed of an IL (with *N*-methyl-*N*-pentylpyrrolidinium (PY_{15}^+), -piperidinium (PI_{15}^+), or -morpholinium (MO_{15}^+) cations and bis(trifluoromethanesulfonyl)imide ($TFSI^-$) anions) and a wide variety of aprotic solvents are reported here to explore the influence of the structure of the cation, solvent, and composition of the mixtures on the properties.

2. EXPERIMENTAL SECTION

Materials. *N*-Methylpyrrolidine (98%), *N*-methylpiperidine (99%), 4-methylmorpholine (99%), and 1-iodopentane (97%) were purchased from Acros Organics. LiTFSI was purchased from 3M. The solvents used are shown in Chart 1. Acetonitrile (AN, 99.8%, anhydrous), diethyl carbonate (DEC, ≥99%, anhydrous), dimethyl carbonate (DMC, ≥99%, anhydrous), ethyl acetate (EA, 99.8%, anhydrous), ethyl butyrate (EB, 99%), ethylene carbonate (EC, 99%, anhydrous), ethyl propionate (EP, 99%), γ-butyrolactone (GBL, ≥99%), γ-valerolactone (GVL, ≥99%), methyl acetate (MA, 99%), methyl butyrate (MB, 99%), methyl isobutyrate (MI, 99%), methyl propionate (MP, 99%), and propylene carbonate (PC, 99.7%, anhydrous) were purchased from Sigma-Aldrich. The water content of each solvent was determined with a Mettler Toledo DL39 Karl Fischer coulometer. All of the chemicals

Received: September 8, 2012
Revised: November 28, 2012
Published: November 29, 2012

   dx.doi.org/10.1021/jp3089403 | J. Phys. Chem. C 2013, 117, 78–84

Chart 1. Chemical Structures of the IL Ions and Solvents Used in This Study

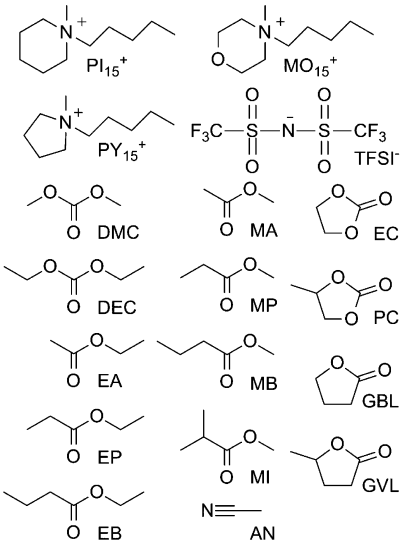

were used as-received, except for the GBL, GVL, MP, MB, MI, EP, EB, and MA solvents which were dried using 3 Å molecular sieves until a water content of less than 30 ppm was measured. The solvents were stored in hermetically sealed bottles in a Vacuum Atmospheres glovebox with an N_2 atmosphere (<10 ppm O_2 and <1 ppm H_2O).

Preparation of ILs and IL–Solvent Mixtures. The desired amines (*N*-methylpyrrolidine, *N*-methylpiperidine, or 4-methylmorpholine) were reacted with 1-iodopentane in EA at a molar ratio of 1.00:0.95 to ensure complete reaction of the haloalkane. The solid iodide salts (i.e., $PY_{15}I$) generated were washed and filtered with EA until the salts were white. The purified salts were then reacted with LiTFSI in water at a molar ratio of 1.00:1.05 to ensure complete reaction of the iodide salt. The resulting ILs (i.e., $PY_{15}TFSI$) separated from the aqueous layer, and the aqueous layer was decanted. The ILs were washed several times with deionized water to remove excess LiTFSI and LiI until the addition of $AgNO_3$ to the wash solution did not form a precipitate. The ILs were then treated with activated carbon until colorless and dried under vacuum at 100 °C for 48 h. The water content was checked with Karl Fischer coulometry and was found to be less than 30 ppm. The purity of the ILs was then verified by ^1H NMR spectroscopy. In addition, Raman spectroscopy is very sensitive to impurities in ILs from the salt synthesis as these generally result in significant fluorescence. Raman spectra of the ILs showed negligible fluorescence. The ILs were stored in hermetically sealed bottles in the glovebox. To prepare the IL–solvent mixtures, stoichiometric amounts of the ILs and solvents were mixed together in the glovebox in hermetically sealed vials.

Thermal Analysis. Differential scanning calorimetry measurements were performed with a TA Instruments Q2000 DSC equipped with a liquid N_2 cooling system. The instrument was calibrated with cyclohexane (solid–solid phase transition at −87.06 °C, melt transition (T_m) at 6.54 °C) and indium (T_m at 156.60 °C). Hermetically sealed Al sample pans were prepared in the glovebox. To ensure complete crystallization, the samples were cycled (5 °C min^{-1}) over a range of temperatures below their T_m until no glass transition (T_g) was observed upon cooling the samples to −150 °C. Only the final DSC heating traces (5 °C min^{-1}) are reported.

Thermogravimetric analysis measurements were performed using a TA Instruments Q5000 TGA. The stability/volatility of the mixtures was measured from ambient temperature to 600 °C under a N_2 atmosphere with a temperature ramp of 5 °C min^{-1}. The samples were removed from the glovebox and transferred to the instrument in a syringe sealed by plunging it into a silicon stopper. The samples were loaded into the TGA pan right before closing the furnace and starting the temperature ramp to limit water contamination and evaporation of the solvents.

Density and Viscosity. Density and viscosity measurements were performed using an Anton-Paar SVM 3000 Stabinger viscometer. The instrument was calibrated using Cannon viscosity (density) standard fluids as follows: 3.689 mPa s^{-1} (0.8150 g cm^{-3}), 50.02 mPa s^{-1} (0.8209 g cm^{-3}), and 1105 mPa s^{-1} (0.8456 g cm^{-3}) at 20 °C. The instrument was initially rinsed with EA, set at 100 °C, and flushed with N_2 gas prior to loading the samples for the measurements. The samples were removed from the glovebox and transferred to the instrument as noted above for the TGA measurements. During the measurements, the inlet and outlet for the instrument were

Table 1. Solvent Properties: Formula Weight, Density, Viscosity, Melting Temperature, Boiling Temperature, Permittivity, Donor/Acceptor Numbers, and Dipole Moment (at 25 °C unless Otherwise Stated)[26–37]

	FW (g mol^{-1})	ρ (g cm^{-3})	η (mPa s^{-1})	T_m (°C)	T_b (°C)	ε	DN	AN	m (D)
EC	88	1.32[c]	1.90[c]	36	238	90.4[c]	16.4		4.87
PC	102	1.20	2.51	−55	242	65.0	15.1	18.3	4.98
GBL	86	1.12	1.73	−44	204	39.1	18.0	18.6	4.12
GVL	100	1.05	2.18	−31	208	36.9[a]			
DMC	90	1.06	0.59	5	90	3.1	15.1		
DEC	118	0.97	0.75	−43	127	2.8	16.0		
MA	74	0.93	0.36	−98	57	6.7	16.5		1.61
MP	88	0.92[a]	0.73	−88	79	5.9[b]			
MB	102	0.90	0.79	−84	103	5.3[b]			
MI	102	0.89	0.75	−84	90		11		
EA	88	0.89	0.44	−84	71	6.0	17.1	1.5	1.88
EP	102	0.89	0.76	−73	99	6.0	17.1		
EB	116	0.88	0.84	−93	120	5.0	16.8		
AN	41	0.78	0.34	−49	82	36.0	14.1	18.9	3.44

[a]At 20 °C. [b]At 35 °C. [c]At 40 °C.

dx.doi.org/10.1021/jp3089403 | J. Phys. Chem. C 2013, 117, 78–84

closed with tight-fitting syringes, and the water content of the samples was checked at the end of the experiments. For all of the samples, the water content was <100 ppm, and for most of them it was <50 ppm range (from Karl Fischer coulometry). The measurements were taken from 20 to 80 °C in 5 °C increments, and then the samples were cooled to 20 °C to verify the initial values (to ensure that no solvent loss occurred during the measurements).

Ionic Conductivity. The conductivity of the mixtures was measured with electrochemical impedance spectroscopy using a Biologic VMP3 potentiostat/galvanostat/EIS. Spectra were collected from 1 MHz to 20 Hz with a 10 mV ac perturbation. AMEL Instruments two-electrode conductivity cells with Pt electrodes were prepared with the samples in the glovebox and then hermetically sealed. Cell constants were determined for each conductivity cell using standard aqueous KCl solutions at 25 °C. Measurements were performed in a Binder environmental chamber from 100 to −40 °C. Temperature steps were 10 °C, and the samples were allowed to equilibrate for at least 45 min after each temperature change before the measurements were taken.

3. RESULTS AND DISCUSSION

The properties of the aprotic solvents used are noted in Table 1. The donor numbers (DNs) are very similar. This is likely due to the fact that all of the solvents (except AN) have a coordinating carbonyl group available. The density of the liquid solvents tends to be higher if the solvents are carbonates instead of esters and if they are cyclic rather than acyclic. The permittivity of the solvents is uniformly low if the solvents are acyclic (whether esters or carbonates), intermediate for the cyclic esters (GBL and GVL), and much higher for the cyclic carbonates (EC and PC). It is interesting to note that there is a significant difference in the permittivity of EC and PC which differ in structure only by the methyl group, whereas the difference between GBL and GVL is minor. The same general trends noted for the permittivity of the solvents are also found for the viscosity with higher permittivity solvents tending to have a higher viscosity (AN is the exception). In addition, solvents with longer alkyl groups generally have a higher viscosity than those with shorter alkyl groups.

Figures 1 and 2 show the thermal phase behavior of the $PY_{15}TFSI$ mixtures with EC and EB, respectively. The $PY_{15}TFSI$–EC mixtures have simple eutectic solid–liquid phase behavior with a eutectic composition of about x = 0.45 (mole fraction of the solvent EC). A significant T_m depression of ~25 °C is thus possible with the addition of a relatively small amount of solvent (a x = 0.50 composition corresponds to a 1/1 mole ratio of IL/solvent). The phase behavior of $PY_{15}TFSI$ with EB is somewhat different. Unlike EC which has a T_m (37 °C) higher than that of the $PY_{15}TFSI$ (11 °C), the T_m of EB is quite low (−97 °C—experimentally found in Figure 2—this differs from the reported value in Table 1). As EB is added to the $PY_{15}TFSI$, the IL melting peak decreases and shifts to lower temperature. A new peak is evident just below −50 °C, but this peak shifted depending upon how the samples were crystallized. This is tentatively assigned to a solvate phase consisting of the IL and EB. It is possible that the shift in the T_m for this phase actually corresponds to two different phases which may crystallize with similar T_m values (a thermodynamically favored IL–solvent phase and an alternative kinetically formed phase with different solvent and ion packing, but perhaps the same composition). The addition of solvent to the IL substantially

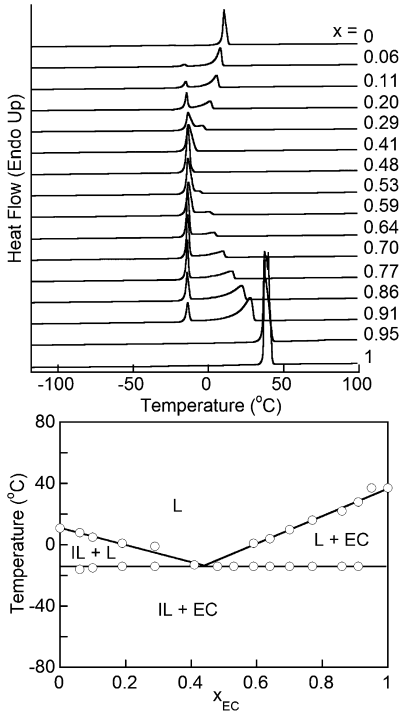

Figure 1. DSC heating traces and the corresponding phase diagram of (1 − x) $PY_{15}TFSI$–(x) EC mixtures (x is mole fraction; phases: EC and IL = crystalline solids, L = liquid).

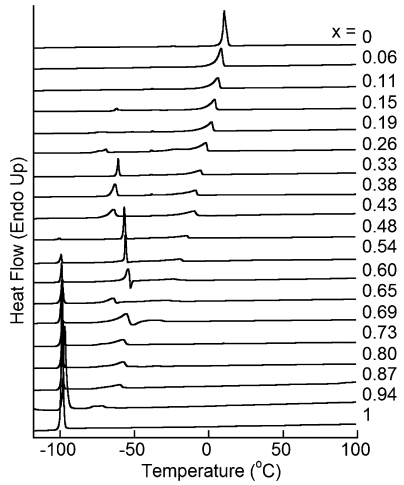

Figure 2. DSC heating traces of (1 − x) $PY_{15}TFSI$–(x) EB mixtures.

extends the temperature range over which the mixtures remain liquid. Other IL–solvent mixtures studied also have similar increases in liquid temperature range at low temperature.

Figure 3 shows the TGA results for the $PY_{15}TFSI$–solvent mixtures with either EC or AN. All of the EC and AN readily volatilize from the mixtures well before their normal boiling point (T_b, Table 1), leaving the pure IL which begins to decompose above 300 °C. The solvents in the mixtures are volatilized at a higher temperature, however, than for the pure solvents. This is likely due to a colligative effect as the surface of the liquids consists principally of nonvolatile ions rather than solvent molecules. The data suggest that the ion–solvent interactions with this IL are relatively weak. Similar IL–solvent mixed electrolytes may thus be constrained by volatility limitations, as for current salt–solvent electrolytes (i.e, 1 M

dx.doi.org/10.1021/jp3089403 | J. Phys. Chem. C 2013, 117, 78–84

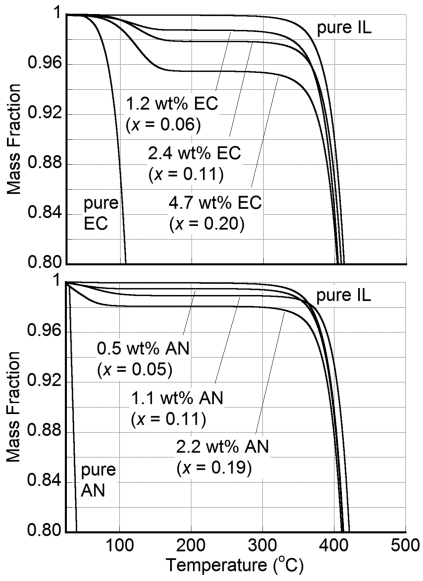

Figure 3. TGA heating traces (5 °C min^{-1}) of the $(1 - x)$ $PY_{15}TFSI-(x)$ solvent (EC and AN) mixtures as well as the pure IL ($PY_{15}TFSI$) and pure solvents. The wt %/mole fraction of the solvents are indicated in the figure.

AN–Et_4NBF_4 mixtures). These results were obtained, however, with an open TGA sample pan with N_2 flow in the furnace. The DSC thermograms (Figures 1 and 2), obtained with hermetically sealed DSC pans, did not show any solvent evaporation up to 100 °C, which should also be the case in a sealed device.

The density variation of the $PY_{15}TFSI$–solvent mixtures is shown in Figure 4. If the data are instead plotted vs weight fraction (not shown), then linear variations are found between the pure $PY_{15}TFSI$ and solvents, as expected. The excess molar volume (V^E) determined from the density data is also shown in Figure 4. The IL mixtures with the four cyclic solvents (i.e., EC, PC, GBL, and GVL) all have relatively small negative V^E values over the entire concentration range. This suggests that solvent molecules with little conformational flexibility do not impact the excess molar volume significantly. In contrast, the mixtures with acyclic solvents result in much larger negative V^E values. A solvent's molecular volume has been correlated with the molecular polarizability.[35] The polarizability values (Å^3) for the acyclic solvents are as follows: AN, 4.4; MA, 7; DMC, 7.6; MP, 8.8; EP, 8.8; EA, 8.9; MB, 10.7; DEC, 11.3 (and EC, 6.6; GBL, 7.9).[36] This suggests that there may be a link between the molecular volume and V^E for the flexible solvent molecules (although AN is not flexible). Similar trends are found for IL–solvent mixtures with $PI_{15}TFSI$ and $MO_{15}TFSI$ ILs (see Supporting Information).

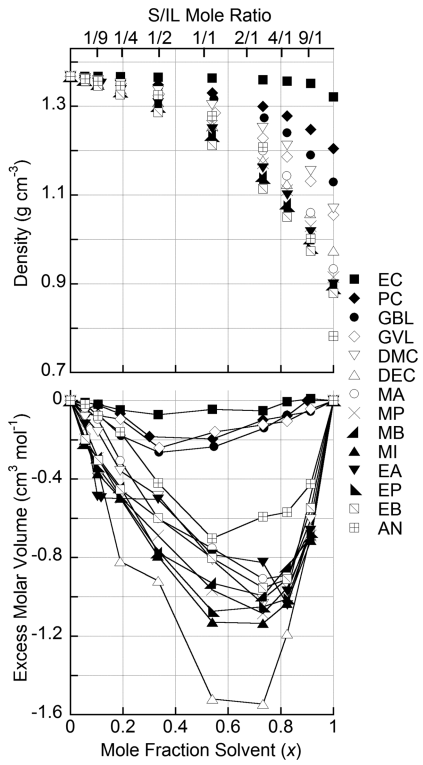

Figure 4. Density and excess molar volume of $(1 - x)$ $PY_{15}TFSI-(x)$ solvent mixtures at 20 °C (data for pure EC at 40 °C). The solvent to IL (S/IL) mole ratio is indicated at the top of the figure.

Figure 5 shows the viscosity data for the $PY_{15}TFSI$–solvent mixtures. A comparison of the data for $x = 1$ (neat solvents at 20 °C) indicates that there is reasonable agreement with the literature values given in Table 1 at 25 °C and these experimentally measured values. Upon solvent addition, even the addition of 5 mol % ($x = 0.05$) solvent results in a substantial decrease in the $PY_{15}TFSI$ viscosity, especially at low temperature. Note that although EC is a solid at ambient temperature, the mixtures with EC remain liquid indefinitely at 20 °C up to 90 mol % ($x = 0.90$) EC. Over the entire concentration range, the tendency of the solvents to affect the viscosity remains relatively constant. Some differences are noted, however, in the ordering for the acetates (i.e., MA and EA) and AN. The difference between the linear carbonates and linear esters decreases as x increases, and the viscosity

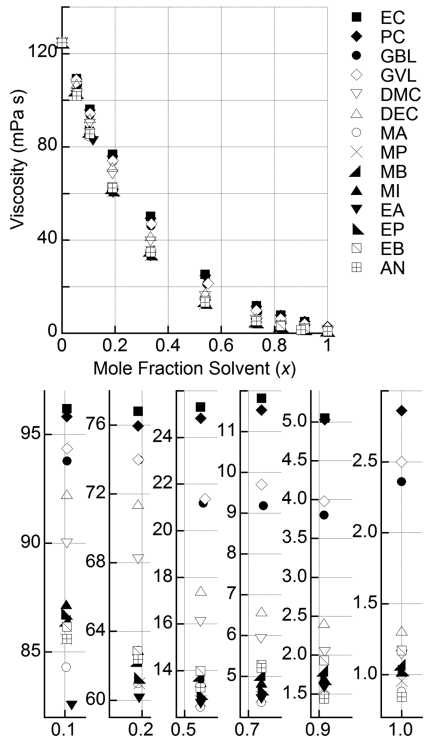

Figure 5. Viscosity of $(1 - x)$ $PY_{15}TFSI-(x)$ solvent mixtures at 20 °C. Bottom plots are expanded sections from the top plot.

dx.doi.org/10.1021/jp3089403 | J. Phys. Chem. C 2013, 117, 78–84

approaches that of the pure solvents. Data for the mixtures at 70 °C are given in the Supporting Information. Data are also provided for IL−solvent mixtures with the $PI_{15}TFSI$ and $MO_{15}TFSI$ ILs. The viscosity of the pure ILs at 20 °C is $PY_{15}TFSI$ (125 mPa s), $PI_{15}TFSI$ (316 mPa s), and $MO_{15}TFSI$ (898 mPa s). The addition of either AN or DMC to the ILs results in a dramatic viscosity reduction up to a solvent mole fraction of about x = 0.5 (1/1 solvent/IL ratio) for all of the ILs. Thereafter, for further additions of solvent, the viscosity values are similar irrespective of the IL for a fixed solvent composition (see Supporting Information).

It has previously been noted that when considering the entire composition range between a mixtures of an IL and molecular solvent, several different regimes may be distinguished.[15,18] For the neat IL, only ions are present. If the cation has a relatively long (butyl or longer) linear alkyl chain, then the charged portions of the cations and anions tend to cluster/interdigitate, leaving the uncharged alkyl chains aggregated together.[19] In the present study, the IL cations have a pentyl alkyl chain. But as solvent is added to an IL, the localized structuring of the ions is impacted. How a solvent molecule interacts with the ions depends upon both the structure of the solvent and its concentration. Nonpolar solvents interact principally with the alkyl chains of the cations, whereas polar solvents interact to a greater extent with the charged portions of the ions.[11,18] For dilute salt concentrations, the solvent molecules far outnumber the ions; the ions thus become dispersed as the solvent molecules shield the ions from one another. The extent to which this dispersion/shielding occurs is dependent upon the strength of the solvent−ion interactions. More polar solvents will therefore disperse the ions (reduce ion aggregation and correlated motion) to a greater extent than less polar solvents.

The variations in the viscosity may be correlated with the solvent's structure. Upon the addition of solvent, the solvent both occupies space and interacts with the ions. As noted previously, the solvents utilized have comparable DN values (Table 1), but due to steric hindrance about the positively charged nitrogen atoms of the cations, strong coordination between the solvent molecules and cations is not expected. Rather, the solvent molecules will direct the carbonyl oxygen atom's (or AN nitrogen atom's) electron lone pair(s) toward these charge centers without the formation of coordination bonds (as occurs for the solvation of alkali metal cations). The permittivity of the solvent may thus be more relevant than the DN for understanding property variations. Addition of the acyclic carbonates (i.e., DMC and DEC), which have the lowest permittivity values (Table 1), results in a lower viscosity reduction than the addition of acyclic esters. Surprisingly, however, the cyclic carbonate (i.e., EC and PC), followed by the cyclic ester (i.e., GBL and GVL), solvents have the highest permittivity values but also the lowest reduction in the viscosity. Other factors than permittivity which are likely critical are the size/shape of the solvent, its conformational flexibility, and the number of electron lone pairs. The latter will have repulsive interactions with anions (and other solvent molecule electron lone pairs) and may, in addition, result in increased (attractive) interactions between a given solvent molecule and multiple neighboring cations (if multiple electron lone pairs are available). Both of these effects will increase the energy barriers for the ions to rearrange themselves (rotational and translational motion) when subjected to shear stress. Notably, AN has a comparable permittivity to that of the cyclic esters (Table 1) but results in a much lower viscosity. This is perhaps surprising as the small size of the solvent would be expected to disrupt (shield) the ion−ion interactions to a lesser extent than for the larger solvent molecules. But AN also has only a single electron lone pair which may therefore result in lower barriers to ion mobility in its vicinity than for the cyclic esters. Multiple factors evidently influence the role that the solvent plays in the viscosity variations of the mixtures.

Figure 6a shows the ionic conductivity of the $PY_{15}TFSI$ mixtures with AN, DMC, GVL, PC, EA, and EP. Several points

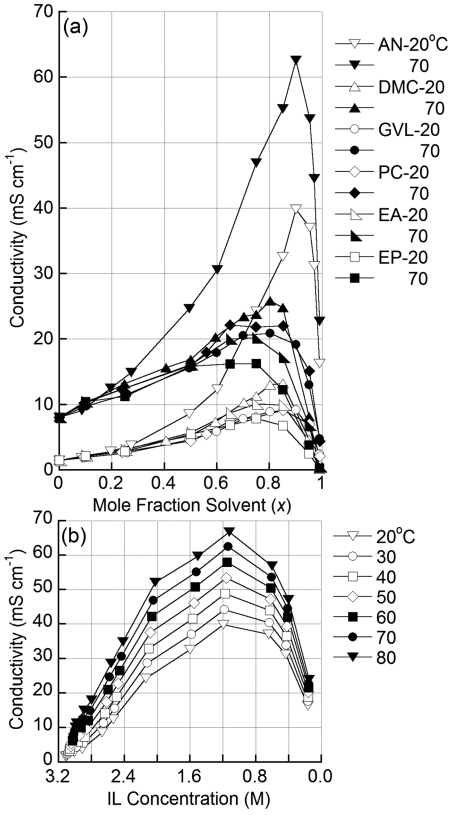

Figure 6. Conductivity of (a) $(1 - x)$ $PY_{15}TFSI$−(x) solvent mixtures vs mole fraction of solvent at 20 and 70 °C and (b) $(1 - x)$ $PY_{15}TFSI$−(x) AN mixtures vs IL concentration; data for the pure IL are on the left.

are notable. For low x values (IL-rich compositions), despite the relatively large differences in viscosity found based upon solvent structure, only minor differences in the conductivity are noted for the different solvents. For higher x values (solvent-rich compositions), variability in the conductivity is found for the different solvents, but this does not correlate well with the viscosity differences noted in Figure 5. A maximum is found for the mixtures between about 1.2 and 2.0 M IL concentration (Figure 6b and Supporting Information), which is similar to the behavior of traditional organic salt−solvent electrolytes. The peak is generally attributed to an increased conductivity due to an increase in the number of charge carriers (upon salt addition to the pure solvent). A further increase in the salt concentration (reduction in x), however, results in a decrease in the conductivity due to increased ion−ion interactions (i.e., ionic association) which reduces both the number of effective charge carriers and their mobility (as is also reflected by the increasing viscosity). The peak shifts to more dilute solutions (higher x values) for the most conductive mixtures. The variation may be linked to both the solvent's permittivity and viscosity, with the

dx.doi.org/10.1021/jp3089403 | J. Phys. Chem. C 2013, 117, 78−84

latter seemingly being more of a factor, as the addition of DMC (low ε and η) results in a somewhat higher conductivity than for GVL (high ε and η), whereas the addition of AN (high ε and low η) results in a dramatic improvement in the conductivity. Data for IL–solvent mixtures with the $PI_{15}TFSI$ and $MO_{15}TFSI$ ILs are provided in the Supporting Information. The conductivity of the pure ILs at 20 °C is $PY_{15}TFSI$ (1.47 mS cm^{-1}), $PI_{15}TFSI$ (0.62 mS cm^{-1}), and $MO_{15}TFSI$ (0.23 mS cm^{-1}). It is interesting to note that, for the three salts, the $PY_{15}TFSI$ mixtures (with AN or DMC) remain more conductive, and the $MO_{15}TFSI$ mixtures less conductive, over the entire concentration range, even for the solvent-rich mixtures (see Supporting Information).

The molar conductivity, Λ (S cm^2 mol^{-1}), is defined as the conductivity, κ (or σ) (S cm^{-1}), divided by the salt concentration, C (mol dm^{-3}): $\Lambda = \kappa/C$. This is a form of normalization of the conductivity in terms of the number of charge carriers. A plot of the molar conductivity (Figure 7) for

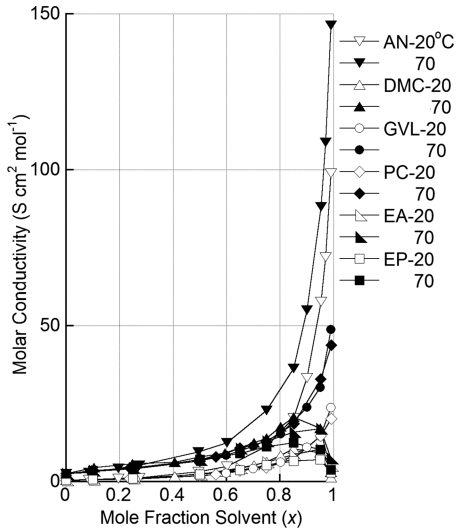

Figure 7. Molar conductivity vs mole fraction of solvent of $(1 - x)$ $PY_{15}TFSI$–(x) solvent mixtures at 20 and 70 °C.

the $PY_{15}TFSI$–solvent mixtures shows very interesting variations. It is worth recalling that the mixtures consist of the same salt (i.e., charge carriers) but different solvents. In particular, in the dilute concentration region (high x), the molar conductivity of the AN mixtures rapidly increases, even though the conductivity itself decreases (Figure 6). This is because the salt (i.e., charge carrier) concentration decreases more rapidly than the conductivity for the AN mixtures. The same trend, although to a lesser extent, is noted for the cyclic solvents GVL and PC. This is not the case, however, for the mixtures with the acyclic carbonate and ester solvents (i.e., DMC, EA, and EP). For the latter mixtures, the molar conductivity peaks as the mixtures become more dilute and then decreases upon further dilution (increasing x).

Explanations for the noted behavior are not immediately evident from the available experimental data, but a computational molecular dynamics (MD) simulation analysis is underway to aid in discerning the origin of the results. Preliminary work (not shown) indicates excellent agreement for the calculated $PY_{15}TFSI$–solvent (with DMC, PC, and AN) conductivity data with the experimental results. The simulations indicate that the degree of ion correlated motion (i.e., tendency for ionic aggregation/clustering)[15,18] is an important factor for the property variations as, for the high x compositions, the DMC mixtures have significant correlated motion which is not the case for the AN and PC mixtures. In fact, the PC mixtures have the least ion correlated motion, as expected due to the much higher permittivity of PC relative to AN and DMC. This indicates that the AN mixtures display a remarkable conductivity (Figure 6) because both the ion–ion interactions are reduced/weakened (relative to the neat IL) and the mobility of the constituent species is high (as exemplified by the low viscosity). In contrast, although the PC mixtures have greatly reduced ion–ion interactions, the mobility of the species is much lower than for the AN mixtures (i.e., a much higher viscosity), whereas for the DMC mixtures, the mobility (perhaps of the solvent—not necessarily the aggregated ions) is relatively high, but the solvent does not effectively break up the ion clusters (i.e., there is significant ion correlated motion). A detailed analysis of the MD simulations will be reported separately to further expand upon this analysis.

4. CONCLUSIONS

The addition of an aprotic solvent to an IL (i.e., $PY_{15}TFSI$, $PI_{15}TFSI$, or $MO_{15}TFSI$) greatly decreases the viscosity of the IL and, up to a certain mole fraction of solvent, increases the conductivity. Furthermore, the addition of solvent can greatly increase the temperature range over which the mixtures remain liquids. The solvent and IL do not appear to interact strongly, however, so that the volatile solvent readily evaporates at elevated temperatures. The properties of the mixtures can be tuned significantly with a judicious choice of both the solvent and the composition (as well as the IL ions).

■ ASSOCIATED CONTENT

Supporting Information

Viscosity data at 70 °C and additional conductivity plots. This material is available free of charge via the Internet at http://pubs.acs.org.

■ AUTHOR INFORMATION

Corresponding Author

*E-mail whender@ncsu.edu.

Author Contributions

§These authors contributed equally.

Notes

The authors declare no competing financial interest.

■ ACKNOWLEDGMENTS

The authors express their gratitude to the U.S. Department of Energy, Office of Basic Energy Sciences, Division of Materials Sciences and Engineering, which fully supported the experimental research under Award DE-DC0001912. The preliminary computational work was partially supported by an Interagency Agreement between the U.S. Department of Energy and the U.S. Army Research Laboratory under DE-IA01-11EE003413 for the Office of Vehicle Technologies Programs including the Batteries for Advanced Transportation Technologies (BATT) Program.

■ REFERENCES

(1) Armand, M.; Endres, F.; MacFarlane, D. R.; Ohno, H.; Scrosati, B. *Nat. Mater.* **2009**, *8*, 621–629.

(2) MacFarlane, D. *The Handbook of Ionic Liquids, Electrochemistry*; Wiley-Interscience: New York, 2009.
(3) Sakaebe, H.; Matsumoto, H. Li Batteries. In *Electrochemical Aspects of Ionic Liquids*; Ohno, H., Ed.; Wiley: Hoboken, NJ, 2011.
(4) Ue, M. Double-Layer Capacitors. In *Electrochemical Aspects of Ionic Liquids*; Ohno, H., Ed.; Wiley: Hoboken, NJ, 2011.
(5) Lex-Balducci, A.; Henderson, W. A.; Passerini, S. Electrolytes for Lithium Ion Battery Materials. In *Lithium Ion Batteries: Advanced Materials and Technologies*; Yuan, Y., Liu, H., Zhang, J., Eds.; CRC Press: Boca Raton, FL, 2011.
(6) Wassersheid, P., Welton, T., Eds. *Ionic Liquids in Synthesis*, 2nd ed.; Wiley-VCH: Weinheim, Germany, 2007.
(7) Yuyama, K.; Masuda, G.; Yoshida, H.; Sato, T. *J. Power Sources* **2006**, *162*, 1401−1408.
(8) Ruiz, V.; Huynh, T.; Sivakkumar, S. R.; Pandolfo, A. G. *RSC Adv.* **2012**, *2*, 5591−5598.
(9) Phung Le, M. L.; Cointeaux, L.; Strobel, P.; Leprêtre, J.-C.; Judeinstein, P.; Alloin, F. *J. Phys. Chem. C* **2012**, *116*, 7712−7718.
(10) Litaiem, Y.; Dhahbi, M. *J. Mol. Liq.* **2012**, *169*, 54−62.
(11) Bardak, F.; Xiao, D.; Hines, L. G., Jr.; Son, P.; Bartsch, R. A.; Quitevis, E. L.; Yang, P.; Voth, G. A. *ChemPhysChem* **2012**, *13*, 1687−1700.
(12) Khupse, N. D.; Kumar, A. *J. Phys. Chem. B* **2011**, *115*, 711−718.
(13) Lopes, J. N. C.; Gomes, M. F. C.; Husson, P.; Padua, A. A. H.; Rebelo, L. P. N.; Sarraute, S.; Tariq, M. *J. Phys. Chem. B* **2011**, *115*, 6088−6099.
(14) Pereiro, A. B.; Deive, F. J.; Rodríguez, A.; Ruivo, D.; Canongia Lopes, J. N.; Esperança, J. M. S. S.; Rebelo, L. P. N. *J. Phys. Chem. B* **2010**, *114*, 8978−8985.
(15) Shimizu, K.; Costa Gomes, M. F.; Pádua, A. A. H.; Rebelo, L. P. N.; Canongia Lopes, J. N. *J. Mol. Struct.* **2010**, *946*, 70−76.
(16) Bayley, P.; Lane, G.; Rocher, N.; Clare, B.; Best, A.; MacFarlane, D.; Forsyth, M. *Phys. Chem. Chem. Phys.* **2009**, *11*, 7202−7208.
(17) Li, W.; Zhang, Z.; Han, B.; Hu, S.; Xie, Y.; Yang, G. *J. Phys. Chem. B* **2007**, *111*, 6452−6456.
(18) Pádua, A. A. H.; Costa Gomes, M. F.; Canongia Lopes, J. N. A. *Acc. Chem. Res.* **2007**, *40*, 1087−1096.
(19) Canongia Lopes, J. N.; Pádua, A. A. H. *J. Phys. Chem. B* **2006**, *110*, 3330−3335.
(20) Jarosik, A.; Krajewski, S. R.; Lewandowski, A.; Radzimski, P. *J. Mol. Liq.* **2006**, *123*, 43−50.
(21) Xu, H.; Zhao, D.; Xu, P.; Liu, F.; Gao, G. *J. Chem. Eng. Data* **2005**, *50*, 133−135.
(22) Diaw, M.; Chagnes, A.; Carré, B.; Willmann, P.; Lemordant, D. *J. Power Sources* **2005**, *146*, 682−684.
(23) Zhang, J.; Wu, W.; Jiang, T.; Gao, H.; Liu, Z.; He, J.; Han, B. *J. Chem. Eng. Data* **2003**, *48*, 1315−1317.
(24) Wang, J.; Tian, Y.; Zhao, Y.; Zhuo, K. *Green Chem.* **2003**, *5*, 618−622.
(25) Seddon, K. R.; Stark, A.; Torres, M.-J. *Pure Appl. Chem.* **2000**, *72*, 2275−2287.
(26) Wu, J.; Lan, Z.; Lin, J.; Huang, M.; Hao, S.; Fang, L. *Electrochim. Acta* **2007**, *52*, 7128−7135.
(27) Marcus, Y. *J. Solution Chem.* **1984**, *13*, 599−624.
(28) Fornefeld-Schwarz, U. M.; Svejda, P. *J. Chem. Eng. Data* **1999**, *44*, 597−604.
(29) Frenkel, M.; Hing, X.; Wilhoit, R. C.; Hall, K. R.; Marsh, K. N. *Densities of Esters and Ethers*; Springer-Verlag: Berlin, Germany, 2001; Vol. *8H*.
(30) Katritzky, A. R.; Chen, K.; Wang, Y.; Karelson, M.; Lucic, B.; Trinajstic, N.; Suzuki, T.; Schüürmann, G. *J. Phys. Org. Chem.* **2000**, *13*, 80−86.
(31) Wypych, G., Ed. *Handbook of Solvents*; ChemTec Publishing: Norwich, NY, 2001.
(32) Riddick, J. A.; Bunger, W. B.; Sakano, T. K. *Organic Solvents: Physical Properties and Methods of Purification*, 4th ed.; John Wiley & Sons, Ltd.: New York, 1986.
(33) Liu, C.-Y.; Ku, H.-C.; Tu, C.-H. *J. Chem. Eng. Data* **1999**, *44*, 360−364.
(34) Thenappan, T.; Devaraj, A. P. *J. Mol. Liq.* **2006**, *123*, 72−79.
(35) Brinck, T.; Murray, J. S.; Politzer, P. *J. Chem. Phys.* **1993**, *98*, 4305−4306.
(36) Bosque, R.; Sales, J. *J. Chem. Inf. Comput. Sci.* **2002**, *42*, 1154−1163.
(37) Barthel, J. M. G.; Krienke, H.; Kunz, W. *Physical Chemistry of Electrolyte Solutions - Modern Aspects*; Springer: Berlin, 1998.